Journal of Molecular and Cellular Cardiology 52 (2012) 741–752

Contents lists available at SciVerse ScienceDirect

Journal of Molecular and Cellular Cardiology

journal homepage: www.elsevier.com/locate/yjmcc

Original article

Carbonic anhydrase XIV in the normal and hypertrophic myocardium

Lorena A. Vargas, Bernardo V. Alvarez *

Centro de Investigaciones Cardiovasculares, Consejo Nacional de Investigaciones Científicas y Técnicas, Facultad de Ciencias Médicas, Universidad Nacional de La Plata, 1900 La Plata, Argentina

ARTICLE INFO

Article history:
Received 11 October 2011
Received in revised form 21 November 2011
Accepted 14 December 2011
Available online 22 December 2011

Keywords:
AE3 Cl^-/HCO_3^- exchanger
Carbonic anhydrase XIV
Cardiomyocyte
Cardiac hypertrophy
Intracellular pH

ABSTRACT

Two AE3 transcripts, full-length (AE3fl) and cardiac (AE3c) are expressed in the heart. AE3 catalyzes electroneutral Cl^-/HCO_3^- exchange across cardiomyocyte sarcolemma. AE proteins associate with carbonic anhydrases (CA), including CAII and CAIV, forming a HCO_3^- transport metabolon (BTM), increasing HCO_3^- fluxes and regulating cardiomyocytes pH. CAXIV, which is also expressed in the heart's sarcolemma, is a transmembrane enzyme with an extracellular catalytic domain. Herein, AE3/CAXIV physical association was examined by coimmunoprecipitation using rodent heart lysates. CAXIV immunoprecipitated with anti-AE3 antibody and both AE3fl and AE3c were reciprocally immunoprecipitated using anti-CAXIV antibody, indicating AE3fl–AE3c/CAXIV interaction in the myocardium. Coimmunoprecipitation experiments on heart lysates from a mouse with targeted disruption of the *ae3* gene, failed to pull down AE3 with the CAXIV antibody. Confocal images demonstrated colocalization of CAXIV and AE3 in mouse ventricular myocytes. Functional association of AE3fl and CAXIV was examined in isolated hypertrophic rat cardiomyocytes, using fluorescence measurements of BCECF to monitor cytosolic pH. Hypertrophic cardiomyocytes of spontaneously hypertensive rats (SHR) presented elevated myocardial AE-mediated Cl^-/HCO_3^- exchange activity (J_{HCO3-} $mM.min^{-1}$) compared to normal (Wistar) rats (7.5 ± 1.3, $n = 4$ *versus* 2.9 ± 0.1, $n = 6$, respectively). AE3fl, AE3c, CAII, CAIV, and CAIX protein expressions were similar in SHR and Wistar rat hearts. However, immunoblots revealed a twofold increase of CAXIV protein expression in the SHR myocardium compared to normal hearts ($n = 11$). Furthermore, the CA-inhibitor, benzolamide, neutralized the stimulatory effect of extracellular CA on AE3 transport activity (3.7 ± 1.5, $n = 3$), normalizing AE3-dependent HCO_3^- fluxes in SHR. CAXIV/AE3 interaction constitutes an extracellular component of a BTM which potentiates AE3-mediated HCO_3^- transport in the heart. Increased CAXIV expression and consequent AE3/CAXIV complex formation would render AE3 hyperactive in the SHR heart.

1. Introduction

The heart is an excitable tissue that requires tight control of the intracellular pH (pH_i). In cardiac muscle, the regulation of pH_i depends on the balance between transporters that load cardiac muscle cells with acid and those that have the effect of extruding acid from the cardiomyocytes [1]. Changes in pH_i directly affect cardiac contractility and development of muscle tension, with a pronounced depression of contractility observed during acidosis of the heart [2]. Thus, deviations of normal pH_i have been implicated in changes of myofilament Ca^{2+} sensitivity [3,4].

Members of the AE family arise from three genes: AE1, AE2, and AE3 [5,6]. The *SLC4A3* gene encodes two AE3 alternate transcripts expressed in cardiac tissues, full length AE3 (AE3fl) and the cardiac AE3 (AE3c) [7]. The AE3 transcripts differ in their N-terminal sequence and molecular mass; AE3c polypeptide is 120 kDa, while AE3fl variant is ~160 kDa. In addition to AE3, AE1 is present in the mouse heart localized at the sarcolemmal membrane of ventricular myocytes [8]. Other Cl^-/HCO_3^- exchangers, members of the SLC26 family, namely SLC26A3 and SLC26A6, have also been detected in the myocardium [9]. In addition, acid loading mechanisms found in the heart involve the putative Cl^-/OH^- exchanger (CHE) which acidifies by efflux of OH^- [10]. AE3 catalyzes electroneutral Cl^-/HCO_3^- exchange across cell membranes, hence regulating $[Cl^-]_i$, $[HCO_3^-]_i$, pH_i, and cell volume [5]. Cl^-/HCO_3^- exchange by AE3 has been well documented in cardiomyocytes [11,12] and is important during normal pH regulation [12], as well as pathological conditions [13–15].

AE3 associates with carbonic anhydrases (CA) II (CAII), IV (CAIV), and IX (CAIX) to form a HCO_3^- transport metabolon, which increases HCO_3^- flux across the plasma membrane [16,17]. Up to date, 16

Abbreviations: AE3fl, Cl^-/HCO_3^- exchanger full length isoform 3; AE3c, Cl^-/HCO_3^- exchanger cardiac isoform 3; SLC26A6, human SLC26 family solute carrier member A6; Slc26a6, mouse SLC26 family solute carrier member A6; CAXIV, carbonic anhydrase isoform XIV; HEK, human embryonic kidney; SLC, solute carrier; pH_i, intracellular pH; BZ, benzolamide (carbonic anhydrase inhibitor); SHR, spontaneously hypertensive rats.

* Corresponding author. Tel./fax: +54 221 483 4833.
E-mail address: balvarez@med.unlp.edu.ar (B.V. Alvarez).

0022-2828/$ – see front matter © 2011 Elsevier Ltd. All rights reserved.
doi:10.1016/j.yjmcc.2011.12.008

members of the CA family differing in their tissue distribution and subcellular localization have been characterized in mammalian cells. Carbonic anhydrases accelerate the reversible hydration of CO_2 to form HCO_3^- and H^+. Lately, CAXIV and AE3 interactions in excitable tissues of the central nervous system (CNS) have been described [18,19]. Both CAXIV and CAIV enhance AE3-mediated Cl^-/HCO_3^- exchange in CNS hippocampal neurons [18].

CAIV, CAIX, and CAXIV are expressed in different subcellular compartments within cardiac myocytes [20], suggesting divergent functions of the enzymes in excitation–contraction coupling. The similar tissue expression pattern and previously reported interaction of AEs and CAs into a HCO_3^- transport metabolon [17–19,21], suggested that AE3 might structurally associate with CAXIV in the heart.

To examine whether AE3 and CAXIV physically associate in the heart, co-immunoprecipitation experiments were performed using rodent (mouse, rat) heart lysates. We found that CAXIV coimmunoprecipitated with anti-AE3 antibody and AE3 could be coimmunoprecipitated using anti-CAXIV antibody.

The hypertrophic myocardium of spontaneously hypertensive rats (SHR) presented elevated AE3-mediated Cl^-/HCO_3^- exchange activity, compensated by enhanced NHE1 Na^+/H^+ exchange activity [14]. This combined action of AE3 and NHE1 results in a net cellular Na^+ loading without changes of pH_i, as observed in cardiomyocytes stimulated with the growth factors angiotensin II (AngII) and endothelin 1 [22,23]. Herein, we observed that the hypertrophic myocardium of SHR presented elevated expression of CAXIV compared to normal hearts. Consistent with this finding, cardiomyocytes from SHR displayed elevated Cl^-/HCO_3^- exchange activity compared to normal cardiomyocytes which was normalized by the poorly membrane-permeant CA blocker, benzolamide.

The results presented in this work indicate that the AE3/CAXIV complex constitutes a system to dispose of high CO_2 waste generated from the continuous contractile activity of the heart and to regulate pH_i, contributing to heart function. Exacerbated AE3/CAXIV complex in SHR could be a leading factor to elicit the hypertrophic growth of the heart.

2. Materials and methods

2.1. Animals

Male spontaneously hypertensive rats (SHR) and age-matched Wistar rats were used. SHR and Wistar rats were originally derived from Charles River Breeding Farms, Wilmington, Mass. All animals were housed under identical conditions and had free access to standard dry meal and water. *ae3* knock-out mice used for this study were produced through targeted mutagenesis, and have been previously described [24]. Protocols that involved rats were reviewed and approved by the Animal Welfare Committee of La Plata School of Medicine and performed in accordance with the Guide for the Care and Use of Laboratory Animals (Argentine Republic Law No. 14346), concerning animal protection.

2.2. Preparation of mouse heart lysates, and HEK293 cell lysates

Mice were sacrificed by an overdose of Euthanyl (sodium pentobarbital). Hearts were rapidly explanted out and placed in 4 ml ice-cold IPB buffer (1% Igepal, 5 mM EDTA, 0.15 M NaCl, 0.5% Deoxycholate, 10 mM Tris–HCl, pH 7.5), containing 2 mg/ml BSA and protease inhibitors (PI, MiniComplete Tablet, Roche). Tissue was disrupted in a Polytron (Kinematica GMBH, Switzerland) and kept on ice for 10 min. HEK293 cells grown on 60 mm Petri dish were disrupted in 250 µl of IPB buffer containing PI, with a cell scraper. Disrupted HEK293 cells were incubated on ice, 10 min.

2.3. Protein expression

Expression constructs for mouse CAXIV [25], rat AE3c [26], rat AE3fl [26], rat AE3–HA [22,27], and human SLC26A6 [9], have been described previously. The V159Y CAXIV mutant construct was a generous gift from Dr. W. Sly (Saint Louis University, MO). HEK293 cells were individually transfected with CAXIV, AE3c, or AE3fl, or AE3–HA, cDNAs, or co-transfected with AE3–HA and CAXIV, or cotransfected with AE3–HA and the CAXIV V159Y mutant, cDNAs, using Lipofectamin 2000™ transfection reagent (Invitrogen, Carlsbad, CA, USA) [28]. Cells were grown at 37 °C in an air/CO_2 (19:1) environment in DMEM medium, supplemented with 5% (v/v) fetal bovine serum and 5% (v/v) calf serum.

2.4. Determination of pH_i changes in HEK293 cells

Untransfected or transfected HEK293 cells were incubated with 10 µg/ml BCECF-AM dye for 20 min at 37 °C. Dye-loaded cells were washed and resuspended in a solution containing (in mM): 5 KCl, 140 NaCl, 1 $MgSO_4$, 1 calcium gluconate, 5 glucose, 25 $NaHCO_3$, 10 Hepes, 2.5 NaH_2PO_4, pH 7.4 (Cl^--containing). Cells were placed into a cuvette in a Cl^--free HCO_3^- buffer solution containing (mM): 5 potassium gluconate, 140 sodium gluconate, 1 $MgSO_4$, 1 calcium gluconate, 5 glucose, 25 $NaHCO_3$, 10 Hepes, 2.5 NaH_2PO_4, pH 7.4, in the presence or absence of the CA inhibitor, benzolamide (BZ, 10 µM). The cell suspension was continuously stirred to prevent cells from settling out. Both buffers were bubbled with 5% CO_2 and 95% O_2. Cl^-/HCO_3^- exchange activity of AE3fl–HA was measured during the alkalinization induced from exposing the cells to the Cl^--free HCO_3^- buffer solution, in the presence of 30 µM EIPA ((5-(N-ethyl-N-isopropyl) amiloride (Sigma)) to block Na^+/H^+ exchanger (NHE) activity. Cell suspensions loaded with BCECF were excited at 503 and 440 nm, and the emitted fluorescence was collected at 535 nm. pH_i was calculated in each preparation using a high K^+-nigericin solution [19]. Initial rate of pH_i change upon exposing the cells to Cl^--free buffer was calculated by fitting a linear regression of the first 1 min of the recorded pH_i immediately after switching the Cl^--containing buffer to Cl^--free buffer (anion exchange assay). HCO_3^- rate (J_{HCO3-} in $mM.min^{-1}$) was estimated as described previously [19]. The transport activity of sham-transfected cells was subtracted from the total rate to ensure that these rates consisted only of AE3–HA transport activity. The relationship between the ratios of fluorescence 503 nm/440 nm and the pH value obtained in each step was linear.

2.5. Isolation of rat heart membranes

Heart membranes were prepared from freshly isolated ventricles of adult SHR and Wistar rats (Table 1), which were separated and homogenized with a Brinkmann Homogenizer (Brinkmann Instruments, Westbury, NY) in 4 ml of ice-cold solution, containing 0.32 M sucrose, 1 mM EGTA, 0.1 mM EDTA, 10 mM Hepes, pH 7.5 and protease inhibitors (Complete Mini protease inhibitor cocktail tablets, Roche, Germany). Homogenates were centrifuged at 1440×*g* for 5 min in a Beckman G5-6K centrifuge. Supernatants were removed and centrifuged at 66,700×*g* for 30 min at 4 °C in a Beckman TLA 100.4 rotor. The resulting membrane fraction was resuspended in 300 µl of PBS containing (mM): NaCl 140, KCl 3, Na_2HPO_4 6.5, KH_2PO_4 1.5, pH 7.5. The Quant-iT protein assay kit (Molecular Probes/Invitrogen Labeling and Detection, Eugene, OR, USA) was used to determine protein concentration on a Qubit fluorometer (Invitrogen) according to the manufacturer's instructions.

2.6. Immunodetection

Two days post-transfection, cells were washed in PBS buffer and cell lysates were prepared by addition of 150 µl SDS-PAGE sample

Table 1
General characteristics of spontaneously hypertensive rats (SHR) and normal rats (Wistar).

SHR (n = 4–12)					Wistar (n = 4–15)				
Age (weeks)	BW (g)	HW (mg)	HW/BW (mg/g)	LVW/BW (mg/g)	Age (weeks)	BW (g)	HW (mg)	HW/BW (mg/g)	LVW/BW (mg/g)
13 ± 1	294 ± 15	1131* ± 29	4.04* ± 0.23	3.17* ± 0.15 (n = 4)	12 ± 1	289 ± 13	814 ± 40	2.89 ± 0.19	1.89 ± 0.02 (n = 4)

n = number of animals; BW = body weight; HW = heart weight; LVW = left ventricular weight. Values are mean ± SEM.
* $p<0.05$ *t*-test.

buffer to 60 mm Petri dish. Heart lysates were prepared by addition of equal volume of SDS-PAGE sample buffer to membrane fractions (300 μl), or to supernatant fractions (2000 μl). Cell samples (50 μg protein), or heart samples (100–250 μg) were resolved by SDS-PAGE on 7.5–10% acrylamide gels, as indicated. Proteins were transferred to PVDF membranes, and then incubated with rabbit anti-AE3 [29] (SA8, 1:2000 dilution), goat anti-CAXIV (N-19, Santa Cruz, CA, USA, 1:500), mouse anti-CAIX antibody [16] (1:1000 dilution), rabbit anti-CAII antibody (H-70, Santa Cruz, CA, USA, 1:1000 dilution), rabbit anti-CAIV antibody (H-50, Santa Cruz, CA, USA, 1:1000 dilution), mouse anti-HA antibody (16B12, Covance, CA, USA, 1:2000 dilution) [22,27], mouse anti-GAPDH antibody (MAB374, Millipore, MA, USA, 1:1000 dilution), or rabbit polyclonal anti-SLC26A6 antibody (1:1000 dilution). Anti-SLC26A6 antibody has been used previously [9]. Immunoblots were then incubated with 1:1000 dilution of donkey anti-rabbit IgG (Santa Cruz, CA), or mouse anti-goat IgG (Santa Cruz, CA, USA), or sheep anti-mouse IgG (NA931V, Amersham Biosciences, UK), conjugated to horseradish peroxidase. Blots were visualized and quantified using ECL reagent and a Kodak Image Station or a Bio-Rad Image Station.

2.7. Coimmunoprecipitation

Homogenates of heart were centrifuged at 1440×*g* for 5 min in a Beckman G5-6K centrifuge. Supernatants (3.5 ml) were removed and applied to 50 μl protein G Sepharose or 50 μl protein A Sepharose (50% slurry) for 3 h at 4 °C. After centrifugation (5 min, 8000×*g*), lysates were incubated overnight with goat polyclonal anti-CAXIV antibody (6 μl, 1.2 μg IgG), or non-immune goat serum (6 μl), or rabbit polyclonal anti-AE3 antibody (5 μl, 1.5 μg IgG), or rabbit anti-AE3c antibody [26] (5 μl, 1.5 μg IgG), and 100 μl protein G Sepharose or 100 μl protein A Sepharose (at 4 °C, overnight). Resin was washed and resuspended in an equal volume of 2× SDS/PAGE sample buffer. Samples were electrophoresed on 7.5% or 10% acrylamide gels, as indicated. Immunoblots were probed with anti-AE3 antibody (SA8, 1:2000 dilutions), rabbit anti-AE3c antibody (1:1000 dilutions), or anti CAXIV antibody (1:500 dilutions).

2.8. Isolation of mouse and rat cardiomyocytes

Adult mice and rats were anesthetized with Euthanyl (100 mg/kg I.P.). Rat or mouse hearts were rapidly removed, and ventricular myocytes obtained by enzymatic dissociation, using standard protocols [8,30].

2.9. Intracellular pH measurements of rat cardiomyocytes

pH_i was measured in single myocytes with an epi-fluorescence system (Ion Optix, Milton, MA), using the previously described BCECF technique [31]. Briefly, myocytes were incubated at room temperature for 30 min with 10 μM BCECF-AM followed by 30 min washout. Dye-loaded cells were placed in a chamber on the stage of an inverted microscope (Nikon TE 2000-U) and alternately superfused with a Cl^--containing solution or a Cl^--free solution, as above, in the presence or absence of the CA inhibitor, benzolamide (BZ, 10 μM). Both buffers were continuously bubbled with 5% CO_2 and 95% O_2. Dual excitation (440–495 nm) was provided by a 75 W Xenon arc lamp and transmitted to the myocytes. Emitted fluorescence was collected with a photomultiplier tube equipped with a band-pass filter centered at 535 nm. The 495-to-440 nm fluorescence ratio was digitized at 10 kHz (ION WIZARD fluorescence analysis software). At the end of the experiment, the fluorescence ratio was converted to pH_i by calibrations using the high K^+-nigericin method [14]. ΔpHi/dt at each pH_i, obtained from an exponential fit of the alkalinization phase (switching from Cl^--containing to Cl^--free buffer) in myocytes from Wistar and SHR rats, was analyzed to calculate the net H^+ efflux (J_{H+}), then $J_{H+} = \beta_{tot}\,\Delta pHi/dt$, where β_{tot} is total intracellular buffering capacity. β_{tot} was estimated in myocytes isolated from Wistar and SHR rats, and was calculated by the sum of the intracellular buffering due to CO_2 (βCO_2) plus the intrinsic buffering capacity (β_i). βCO_2 was calculated as, $\beta CO_2 = 2.3\,[HCO_3^-]_i$, where $[HCO_3^-]_i = [HCO_3^-]_o\,10^{pHi-pHo}$ [12,32]. β_i of the myocytes was measured by exposing cells to varying concentrations of NH_4Cl in Na^+-free Hepes bathing solution. pH_i was allowed to stabilize in Na^+-free solution before application of NH_4Cl. β_i was calculated from the equation $\beta_i = \Delta[NH_4^+]_i/\Delta pH_i$ and referred to the mid-point values of the measured changes in pH_i. β_i at different levels of pH_i was estimated from the least squares regression lines β_i vs. pH_i plots.

2.10. Double immunostaining of mouse cardiac myocytes

Single freshly-dissociated myocytes were plated onto 22×22-mm laminin (25–50 μg/ml)-coated glass coverslips and incubated at 37 °C for 30 min to allow attachment. Cells were rinsed, fixed, and permeabilized, as previously [8]. Myocytes were incubated with a combination of primary rabbit anti-CAXIV antibody (H-107, Santa Cruz, CA, USA) and goat anti-vinculin antibody (N-19, Santa Cruz, CA, USA), a combination of goat anti-CAXIV antibody and rabbit anti-α-actinin antibody (H300, Santa Cruz, CA, USA), or a combination of goat anti-CAXIV antibody and rabbit anti-mouse AE3 (AP3) [8]. Combined primary antibodies were used at 1:100 dilutions. Secondary chicken anti-rabbit conjugated to Alexa fluor 488 and chicken anti-goat conjugated to Alexa fluor 594 was used at 1:200 dilutions. Coverslips were washed in PBS (3×) containing 0.2% gelatin and in PBS (2×), mounted, and viewed with a confocal microscope.

2.11. Imaging and analysis by confocal microscopy

Immunostained isolated cardiomyocytes on coverslips were mounted in Prolong Anti-fade solution containing Dapi for nuclei staining (Molecular Probes, OR, USA). Cardiomyocytes on coverslips were imaged with a Zeiss LSM 510 laser scanning confocal microscope imaging system mounted on an Axiovert 100 M controller. Images were collected using an oil immersion 63× objective (numerical aperture 1.4, plan Apochromat) at a resolution of 0.5–0.7 μm field depth. Filtering was used to integrate the signal collected over 4 frames to decrease noise (scan time = 7 s/frame). Images were analyzed using the Image-Pro Plus software (colocalization tool) colocalization statistics were presented as Pearson's Correlation values (between 0 and 1), as previously [33].

2.12. Statistics

Data are expressed as mean ± SEM. Student's *t*-test or one-way ANOVA followed by Newman–Keuls Multiple Comparison post-test analysis, when appropriate, were used to compare data. $p<0.05$ was considered of statistical significance.

3. Results

3.1. AE3 Cl^-/HCO_3^- exchanger and CAXIV physical association

We assessed the physical interaction between AE3 and CAXIV in the mouse heart, by coimmunoprecipitation. Mammalian hearts express two different AE3 isoforms, AE3fl and AE3c [34]. AE3c and AE3fl isoforms are broadly expressed across the population of ventricular myocytes, but within myocytes, AE3c and AE3fl localize to sarcolemma (SL), T-tubules, and sarcoplasmic reticulum (SR) to some extent [8]. Lysates of mouse cardiac ventricle were immunoprecipitated with goat anti-CAXIV antibody, resolved by SDS/PAGE and probed with a rabbit anti-AE3 C-terminus antibody, which recognizes both AE3c and AE3fl isoforms on immunoblots (Fig. 1). Goat anti-CAXIV antibody was able to precipitate AE3c and AE3fl isoforms from wild-type mouse heart lysates (Fig. 1A), while no AE3 isoforms were detected (anti-AE3 antibody) or immunoprecipitated (anti-CAXIV antibody) from cardiac lysates obtained from $ae3^{-/-}$ null mouse. Similarly, non-immune goat serum was ineffective in immunoprecipitating AE3 with CAXIV from mouse hearts (Fig. 1A), demonstrating specificity of the AE3/CAXIV interaction. Expression of CAXIV in $ae3^{+/+}$ and $ae3^{-/-}$ mouse hearts was similar, as judged on immunoblots (Fig. 1B). Lysates obtained from HEK293 cells transfected with empty vector (pcDNA3) and CAXIV, cDNAs, were also blotted and used for negative and positive controls, respectively (Fig. 1B). Similarly, AE3c and AE3fl isoforms were immunoprecipitated with anti-CAXIV antibody from rat heart lysates (Suppl. Fig. 1).

Reciprocal AE3/CAXIV coimmunoprecipitation experiments were conducted using mouse ventricular lysates (Fig. 2). Both, Anti-AE3 (AP3) antibody, a polyclonal antibody directed against the common C-terminus of the AE3 variants, and cAE3-1, a polyclonal antibody which recognizes only the AE3c variant [26] (Fig. 2A), were able to precipitate CAXIV from wild-type mouse heart (Fig. 2B). AP3 or cAE3-1 antibodies failed to immunoprecipitate CAXIV from cardiac lysates obtained from $ae3^{-/-}$ null mice (Fig. 2B). CAXIV was equally expressed in heart lysates of $ae3^{+/+}$ and $ae3^{-/-}$ mouse (Fig. 2B). AE3fl and AE3c variants were detected in heart lysates prepared from $ae3^{+/+}$ wild-type mouse, but not in lysates prepared from

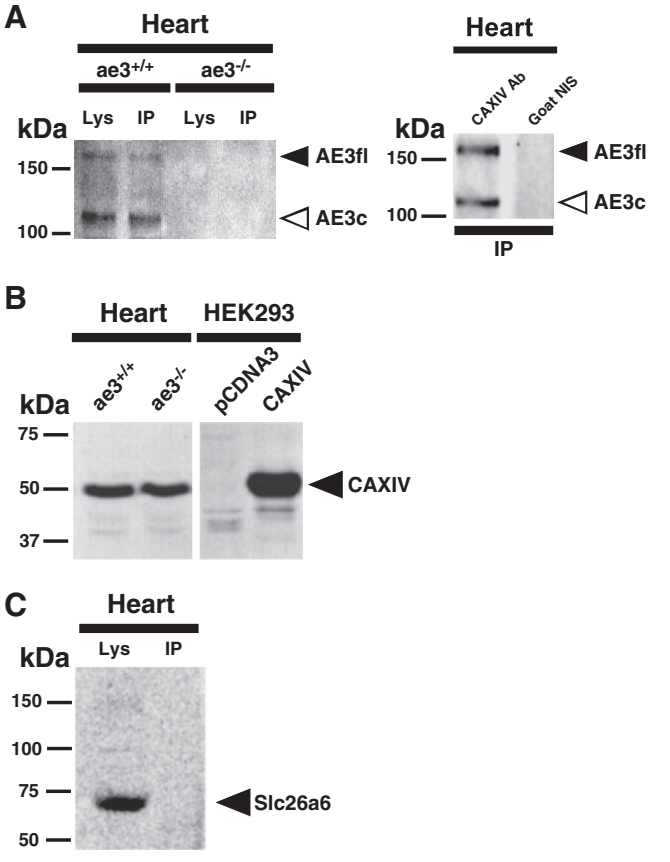

Fig. 1. AE3 and CAXIV physical association in the heart. A, Total heart lysates (Lys) from $ae3^{+/+}$ or $ae3^{-/-}$ mice were immunoprecipitated (IP) with goat polyclonal antibody directed against CAXIV (left panel). Lysates from $ae3^{+/+}$ mouse heart were immunoprecipitated with anti-CAXIV antibody, or goat preimmune serum (right panel). Samples were electrophoresed on 7.5% acrylamide gels, transferred to a PVDF membrane, and probed with rabbit polyclonal anti-AE3 antibody (SA8). AE3fl and AE3c isoforms are indicated by filled and empty arrows, respectively. B, Lysates, prepared from mouse hearts (genotype indicated) or HEK293 cells transfected with vector (pcDNA3), or CAXIV, cDNA, were analyzed on 10% acrylamide gels, transferred to PVDF membranes, and probed with anti-CAXIV antibody. Position of CAXIV is shown (arrow). Samples were resolved on the same gel. C, Lysates prepared from wild type mouse hearts were immunoprecipitated (IP) with antibody directed against CAXIV. Samples were electrophoresed on 8.0% acrylamide gels, transferred to a PVDF membrane, and probed with anti-Slc26a6 antibody. Position of Slc26a6 is shown (arrow).

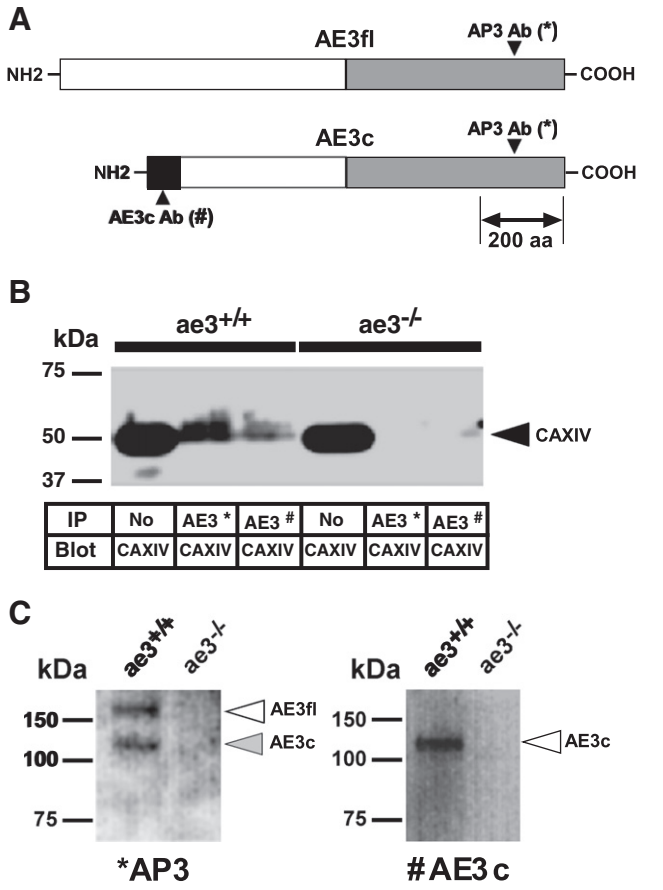

Fig. 2. Immunoprecipitation of AE3/CAXIV complex from mouse ventricles. A, Diagram of the AE3fl and AE3c transcripts with the regions recognized by anti-AE3 antibodies, used for immunoprecipitation experiments. B, Left ventricular lysates of $ae3^{+/+}$ or $ae3^{-/-}$ mice were immunoprecipitated (IP) with anti-AE3 antibody (AP3, AE3*), or anti-AE3c antibody (AE3c#), or were directly loaded onto the gel with no-immunoprecipitation (No). Samples were electrophoresed on 10% acrylamide gels, transferred to PVDF membrane, and probed with anti-CAXIV antibodies (blot), as indicated. Lysates = 50 µl of heart lysate; IP = 50 µl, corresponding to 1.75 ml of heart lysate. Position of CAXIV is shown. C, Samples of the lysate were probed to indicate total amount of input AE3fl and AE3c in each sample, with anti-AE3 antibody (*AP3), or anti-AE3c antibody (#AE3c). Position of AE3fl and AE3c is indicated with open and filled arrows, respectively.

ae3$^{-/-}$ null mouse, using AP3 and cAE3-1 antibodies (Fig. 2C). Hence, CAXIV forms a complex with the two AE3 isoforms expressed in the adult mouse heart, AE3fl and AE3c.

Additional coimmunoprecipitation experiments were repeated in the presence of BZ, to validate the functional role of the AE3/CAXIV interaction in the myocardium (Suppl. Fig. 2). Rat heart lysates were incubated for 20 min in the presence of 10 μM BZ, or incubated for 20 min with vehicle. Samples were immunoprecipitated with anti-AE3 antibody, or without antibody, and the immunoblots revealed with anti-CAXIV antibody (Suppl. Fig. 2A). CAXIV bound AE3, and this interaction was not reduced by 10 μM BZ; lysate/IP ratio of 0.34 ± 0.15 pixels for CAXIV without BZ and 0.32 ± 0.04 pixels with BZ (Suppl. Fig. 2B, $n = 4$). This confirms that the membrane impermeable CA inhibitor, BZ did not disrupt the AE3/CAXIV interaction.

Members of the Slc4a family (AE1, AE2 and AE3) have been detected in cardiac tissues [8,35]. More recently, Slc26a6, a dual Cl^-/HCO_3^- and Cl^-/OH^- exchanger and member of the Slc26a family, was identified as the predominant anion exchanger of the mouse myocardium [9]. Slc26a6 has a similar localization with AE3, with ventricular myocyte labeling at the sarcolemma (SL) and the transverse tubular system (T-tubule), as assessed by immunofluorescence studies [8]. Slc26a6 was also found to interact with cytoplasmic CAII to form a HCO_3^- transport metabolon (BTM) [36], like other AEs [17]. Due to its relevance regarding expression, localization, and

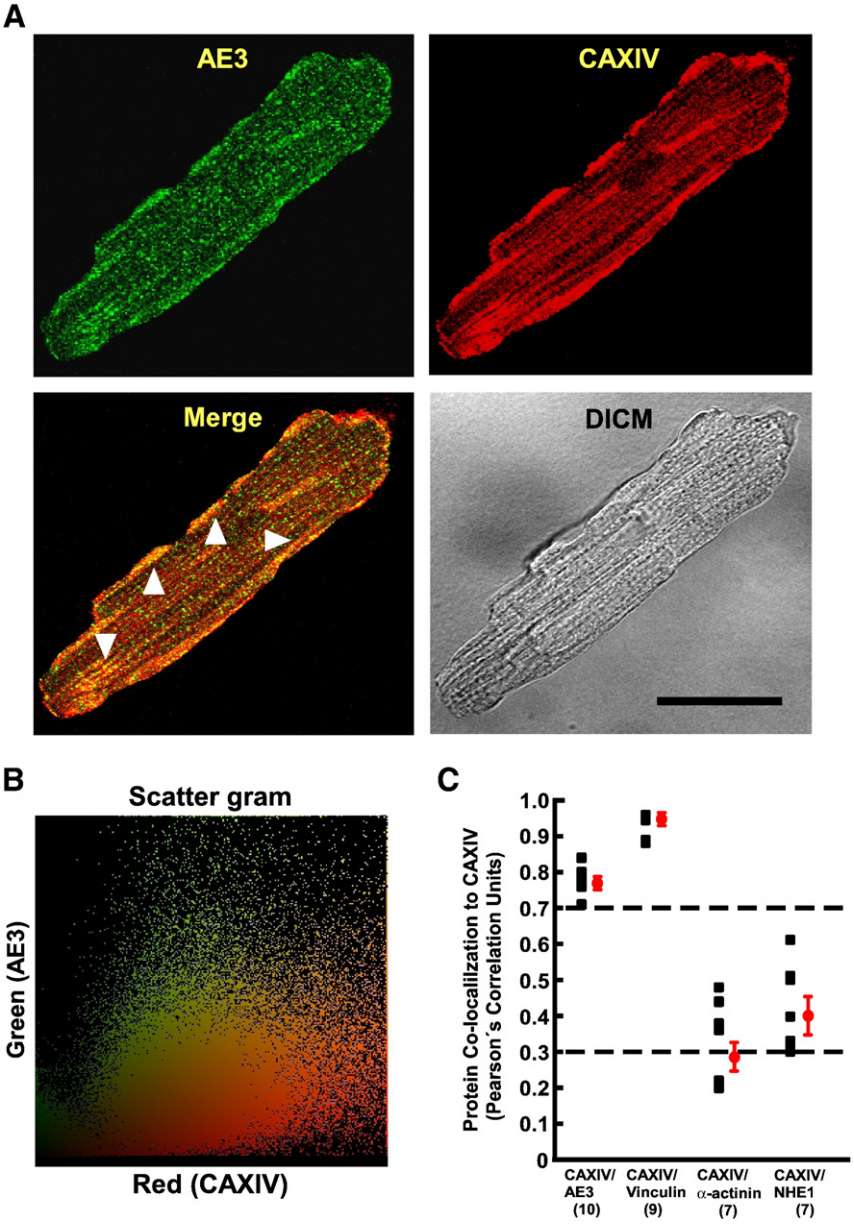

Fig. 3. Localization of CAXIV and AE3 in adult mouse cardiomyocyte. A, Adult mouse cardiomyocyte double-stained with rabbit anti-AE3 antibody (green) and goat anti-CAXIV antibody (red), as indicated in the panels. Immunofluorescence signals were visualized by an Alexa fluor 488-conjugated anti-rabbit IgG antibody (green), and Alexa fluor 594-conjugated anti-goat IgG antibody (red). Images were collected with a Zeiss LSM 510 laser-scanning confocal microscope, with a ×63/1.4 oil immersion objective. Colocalization of AE3 and CAXIV is indicated as merge and with yellow staining. Cardiomyocyte sarcolemmal labeling indicates colocalization of AE3 and CAXIV in a restricted pattern (arrows). DICM, Differential interference contrast microscopy. Scale bars are 30 μm. B, Scatter gram plot indicates fluorescence intensity of both green and red channel signals corresponding to the entire cardiomyocyte merge image (A, merge). Plot diagonal (yellow) indicates colocalization between AE3 (green) and CAXIV (red) signals. C, Colocalization degree of AE3, vinculin, and α-actinin with CAXIV protein performed with the image analysis software Image Pro Plus. Values represent Pearson's Correlation units (r) that reveal the degree of association of pixels of confocal images (n, number of cells analyzed).

activity in cardiac cells, and since Slc26a6 has the ability to transport HCO_3^- ions; we explored the possible association of Slc26a6 and CAXIV, by coimmunoprecipitation experiments. Lysates of mouse ventricle were incubated with goat anti-CAXIV antibody, resolved by SDS/PAGE and immunoblotted with an anti-Slc26a6 antibody (Fig. 1C). Slc26a6 was identified as a single strong band of ~70 kDa in mouse heart lysates. CAXIV antibody, however, failed to immunoprecipitate Slc26a6 protein. Together these data suggest that CAXIV and AE3 form a physical complex, but Slc26a6 does not associate with CAXIV in heart.

3.2. Expression and colocalization of AE3 and CAXIV in isolated adult mouse cardiomyocytes

To examine the role of the AE3/CAXIV complex in hearts, we performed immunofluorescence and confocal microscopy analysis of mouse cardiomyocytes (Fig. 3). An anti-AE3 antibody, which recognized both full-length AE3 and cardiac variants, found AE3 localized at SL and intracellular structures in heart sections and isolated mouse cardiomyocytes [8]. Moreover, AE3 was specifically located to the SL invaginations, the T-tubules and the main Ca^{2+} storage compartment of cardiac cells, the SR. Interestingly, CAXIV has been predominantly localized in the longitudinal SR and in the SL of mouse cardiomyocytes by immunofluorescence, suggesting that CAXIV is crucial for the EC coupling [20]. Merged images suggest extensive colocalization of AE3 and CAXIV in SL membranes of mouse cardiomyocytes (Fig. 3A, yellow). Conversely, AE3 and CAXIV colocalize weakly in intracellular structures, suggesting that AE3 and CAXIV are specifically located in different compartments within the SR and the T-tubule systems. Specificity of the AE3, and CAXIV signals was shown by the absence of signal in isolated cardiomyocyte samples treated with secondary antibody and no primary antibody (not shown). Quantification analysis was performed in cardiomyocytes double-labeled with anti-AE3 and anti-CAXIV antibodies. Scatter gram image shows high degree of overlapping (yellow) between AE3 (green) and CAXIV (red) pixels, suggesting colocalization of both proteins (Fig. 3B). Quantification of the colocalization of green channel pixels (AE3) with red channel pixels (CAXIV) was performed using the Image-Pro Plus software. The degree of association of AE3 with CAXIV is depicted as a Pearson's Correlation coefficient (r) (Fig. 3C) where the r-values between -0.3 ± 0.3 indicate little or no association, $+0.3 \pm 0.7$ weak positive association, and $+0.7 \pm 1.0$ strong positive association. We found that CAXIV shows a high degree of colocalization with CAXIV ($r = 0.77 \pm 0.01$, $n = 10$; Fig. 3C). CAXIV/Vinculin and CAXIV/α-actinin colocalization were also quantified in isolated cardiomyocytes (not shown). CAXIV showed strong colocalization with Vinculin ($r = 0.94 \pm 0.01$, $n = 9$), but weak colocalization with α-actinin ($r = 0.29 \pm 0.06$, $n = 7$) (Fig. 3C). Additionally, colocalization of CAXIV and the plasma membrane NHE1 Na^+/H^+ exchanger was quantified in rat cardiomyocytes (not shown), and the Pearson's Correlation coefficient revealed a weak positive association of the transporter and the CA ($r = 0.40 \pm 0.05$, $n = 7$) (Fig. 3C). We conclude that AE3 and CAXIV strongly colocalize in cardiomyocyte SL. Taken together, these results suggests that the AE3 Cl^-/HCO_3^- exchanger and the transmembrane CAXIV are physically coupled, forming an extracellular component of BTM in the heart. However, the resolution of the optic system used here is not high enough to ultimately demonstrate physical association between AE3 and CAXIV.

3.3. Expression of carbonic anhydrases in the hypertrophic myocardium

We wanted to study the expression of the different CAs to evaluate whether the CA genes could be altered in the pathological heart. To quantify the level of CA protein expression in hearts, immunoblots were performed, which revealed the expression levels of the CAs, namely CAII, CAIV, CAIX, and CAXIV, in hypertrophic and normal rats. Table 1 shows values of heart mass, and heart weight-to-body weight (HW/BW) index, and left ventricular weight-to-body weight (LVW/BW) index of 3–3.5 month-old hypertrophic (SHR) and normal (Wistar) rats. Hearts from SHR exhibited myocardial hypertrophy, as shown by the elevated heart mass, and increased HW/BW and LVW/BW ratios. Ventricles were isolated and lysates of whole ventricles and lysates of membrane fractions prepared to evaluate the expression of intracellular CAII, and membrane-anchored CAIV, respectively. Expression of CAII and CAIV was quantified by densitometry of the immunoblots and was corrected for loading differences by normalization to α-tubulin levels (CAII), or Na^+/K^+ ATPase levels (CAIV) (Fig. 4A). CAII expression did not change in the hypertrophic myocardium of SHR compared to normal (Fig. 6B). Additionally, CAIV expression was slightly reduced in SHR compared to Wistar ($p = 0.133$) (Fig. 4B). Transmembrane CAIX and CAXIV localized in different regions along the SR cardiomyocyte membrane [20]. CAXIV also localized in the SL of cardiomyocytes [20]. Expression of CAIX (not shown) and CAXIV was examined in membrane ventricular lysates of SHR and Wistar rats, on immunoblots (Fig. 5A). CAIX expression was comparable in SHR and control rats (data not shown). Conversely, CAXIV expression increased more than twofold in the hypertrophic hearts (Fig. 5B). CAII, CAIV, and CAXIV protein could be clearly identified on immunoblots with a migration position consistent with the known molecular weight of the proteins (Figs. 4 and 5), and the

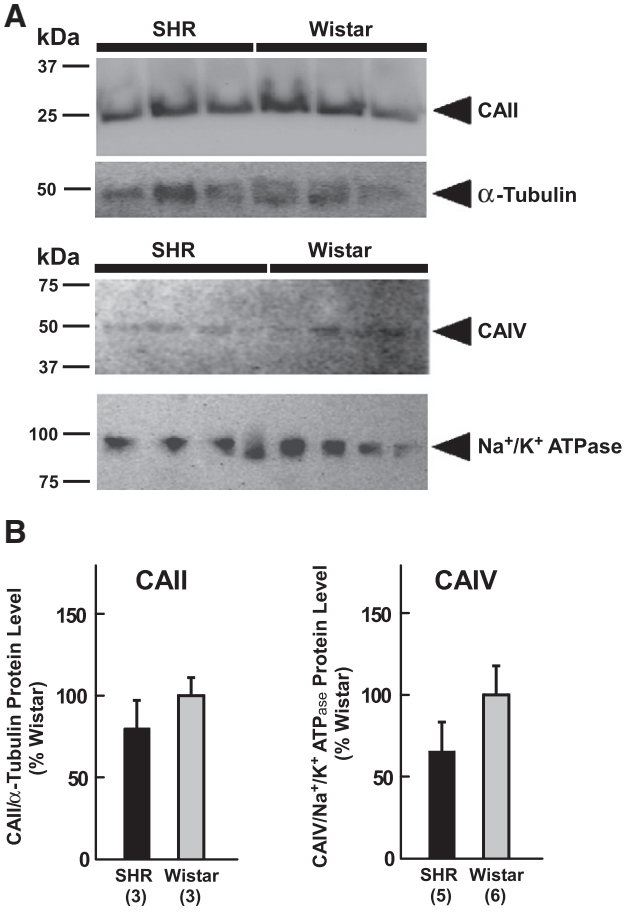

Fig. 4. Expression of CAII and CAIV proteins in adult SHR and Wistar rat hearts. A, Whole lysates (CAII), or membrane lysates (CAIV) were prepared from hypertrophic (SHR) or normal (Wistar) adult rat heart ventricles. Protein samples (100 μg) were subjected to SDS-PAGE analysis, transferred to PVDF membrane, and probed with anti-CAII and anti-α-tubulin antibodies (top panel), and anti-CAIV and anti-Na^+/K^+ ATPase antibodies (bottom panel). Filled arrow indicates position of protein. B, Summary of the normalized protein values expressed relative to the Wistar heart protein expression. Bracket at the bottom indicates the number of hearts analyzed.

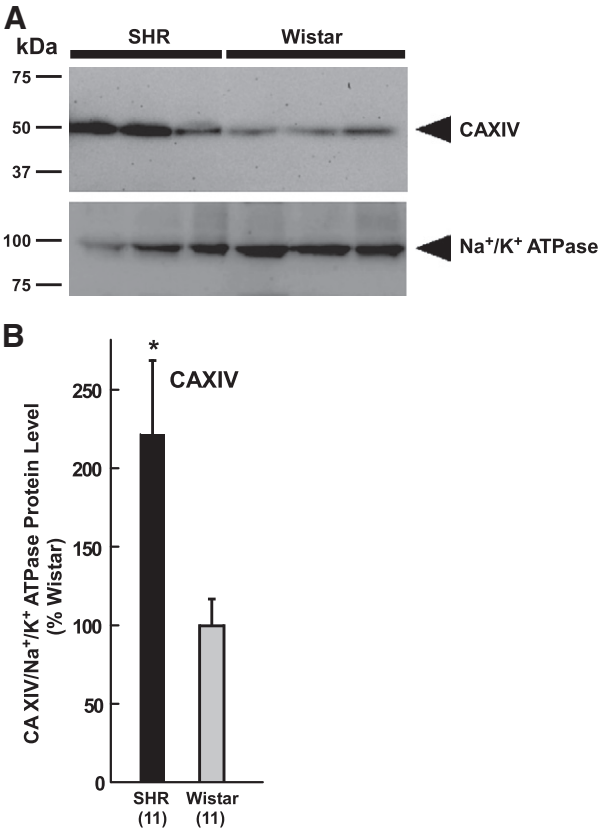

Fig. 5. Expression of transmembrane CAXIV protein in adult SHR and Wistar rat hearts. A, Membrane lysates were prepared from hypertrophic (SHR), or normal (Wistar) adult rat heart ventricles. Protein samples (200 μg) were subjected to SDS-PAGE analysis, transferred to PVDF membrane, and probed with anti-CAXIV (top) and anti-Na^+/K^+ ATPase (bottom) antibodies. Filled arrow indicates position of protein. B, Summary of the normalized protein values expressed relative to the Wistar heart protein expression. Bracket at the bottom indicates the number of heart analyzed. *$p<0.05$, *t*-test.

positive control of CAII, CAIV, and CAXIV, corresponding to HEK293 cells transfected with their respective cDNAs (not shown).

We conclude that only the expression of the CAXIV protein, which forms a BTM complex with AE3, is increased in the hypertrophic hearts of SHR.

3.4. Functional role of the AE3/CAXIV complex in the SHR myocardium

Enhanced activity of the AE3 Cl^-/HCO_3^- exchanger has been reported in the hypertrophic myocardium of SHR [14]. Increased activity of AE3 was accompanied by reduced mRNA expression of the primary AE3 heart transcript, AE3c, and increased mRNA expression of the AE3fl splicing variant, in the hypertrophic myocardium of SHR rats compared to WKY rats, without changes in the mRNA expression of the other AE isoform (AE1, AE2) [37]. Therefore, the overall AE expression in hypertrophic SHR is comparable to non-hypertrophic rats [37]. We considered whether the increased Cl^-/HCO_3^- exchange by AE3 in SHR could arise from the increased CAXIV expression (Fig. 5) and consequent augmented AE3/CAXIV complex formation in the hypertrophic heart. Single freshly isolated rat cardiomyocytes of SHR and Wistar were loaded with the pH-sensitive dye BCECF-AM and perfused alternately with Ringer buffer containing 140 mM NaCl and Ringer buffer lacking Cl^- (Fig. 6). Bicarbonate transport in SHR and Wistar rat cardiomyocytes was monitored by measurements of pH_i upon changes of the transmembrane $[Cl^-]$ gradient (Fig. 6A). pH_i values, recorded during the first minute after Cl^- removal were used to estimate the initial rate of alkalinization induced by reversal of AE activity and fitted to a straight line. Fluxes were estimated at similar pH_i in cardiomyocytes from SHR (7.32 ± 0.02, $n=4$) and Wistar rats (7.29 ± 0.17, $n=6$), and the calculated buffer capacity (β_{tot}) (see Materials and methods) was also comparable in SHR (62 ± 8, $n=4$) and Wistar (61 ± 11, $n=4$). Net HCO_3^- fluxes determined as $J_{HCO3-}=\beta_{tot}\ \Delta pHi/dt$ were higher in SHR (7.5 ± 1.3 mM.min^{-1}, $n=4$) compared to Wistar (2.9 ± 0.1 mM.min^{-1}, $n=6$) (Fig. 6B). The role of CA in determining the rate of AE-mediated Cl^-/HCO_3^- exchange activity in SHR and Wistar myocytes was studied in the absence and presence of benzolamide (BZ, 10 μM), a CA inhibitor with reduced membrane permeability [18,38–40]. Previously, BZ was found to decrease the AE3-mediated CAXIV-dependent HCO_3^- fluxes in hippocampal neurons [18]. Interestingly, in myocytes of SHR pre-incubated (20 min) with BZ, the HCO_3^- fluxes were significantly reduced (3.7 ± 1.5 mM.min^{-1}, $n=3$). Benzolamide also diminished HCO_3^- fluxes in the control myocardium of Wistar rats (1.2 ± 0.2 mM.min^{-1}, $n=4$), proving the dependence upon extracellular CA of Cl^-/HCO_3^- exchange by AE3 in the normal myocardium (Fig. 6B). HEK293 cells express endogenous CAII and the binding of CAII to transfected AE3 increases the HCO_3^- fluxes mediated by the AE3 Cl^-/HCO_3^- exchanger [19,21]. Interestingly, BZ did not significantly alter the Cl^-/HCO_3^- exchange activity by AE3fl–HA, 3.7 ± 1.1 mM H^+.min^{-1} ($n=11$) in the absence of BZ, versus 2.7 ± 0.7 mM H^+.min^{-1} ($n=7$) in the presence of BZ, when AE3fl–HA was transiently expressed in the HEK293 cell expression system (Fig. 7). Thus, BZ did not affect the CAII–AE3fl–HA interaction demonstrating a poor permeability of the CA inhibitor at the dose used herein.

Since changes of AE3 protein expression could affect the AE3-mediated HCO_3^- flux in the hypertrophic myocytes, we analyzed the expression of AE3fl and AE3c in SHR and Wistar whole ventricular lysates, by immunoblots (Figs. 6C, D). AE3c and AE3fl protein expressions were quantified by densitometry of the immunoblots and values were corrected for loading differences by normalization to glyceraldehyde 3-phosphate dehydrogenase (GAPDH) levels. Each of the proteins could be clearly identified on immunoblots with a migration position consistent with the known molecular weight of the protein (Fig. 6C). AE3c expression did not change significantly in SHR hearts ($93\pm10\%$, $n=5$), compared to normal hearts ($100\pm21\%$, $n=4$) ($p=0.75$) (Fig. 6D). In addition, AE3fl protein levels were slightly reduced in hypertrophic ($83\pm7\%$, $n=5$), compared to normal rat hearts ($100\pm11\%$, $n=4$) ($p=0.34$) (Fig. 6D). Total AE3 Cl^-/HCO_3^- exchanger protein level (the sum of AE3c and AE3fl) was also quantified in SHR and Wistar ventricular lysates, and AE3 total did not change significantly in hypertrophic ($87\pm5\%$, $n=10$) compared to normal ventricles ($100\pm12\%$, $n=8$) ($p=0.33$) (Fig. 6D).

From these experiments we conclude that the increased rate of AE-mediated Cl^-/HCO_3^- exchange activity observed in hypertrophic SHR cardiomyocytes is not attributable to modification in the AE3 protein expression levels.

To further explore the effect of CAXIV on AE3-mediated Cl^-/HCO_3^- exchange activity, HEK293 cells were transiently transfected with AE3fl–HA cDNA, or cotransfected with AE3fl–HA and CAXIV, cDNAs, and the expression of AE3fl–HA and CAXIV analyzed on immunoblots (Fig. 7A). For functional assays transfected cells were resuspended and maintained in a Ringer's buffer containing Cl^-, placed into a cuvette perfused with a Ringer buffer lacking Cl^-. HCO_3^- transport was monitored by measurements of pH_i upon changes on transmembrane $[Cl^-]$ gradient (Figs. 7B and C). Transport rates were corrected for the abundance of total AE3fl–HA protein expression on immunoblots (not shown). Coexpression of AE3fl–HA with CAXIV significantly increased AE3-mediated HCO_3^- transport activity by 100% (7.4 ± 2.0 mM H^+.min^{-1}, $n=14$), compared to cells transiently expressing AE3fl–HA alone (Fig. 7C). The role of CAXIV in determining the rate of Cl^-/HCO_3^- exchange activity by AE3 was studied in the absence and presence of BZ. CA inhibitors do not act directly on the Cl^-/HCO_3^- exchanger itself, but instead mediates their effects on CA

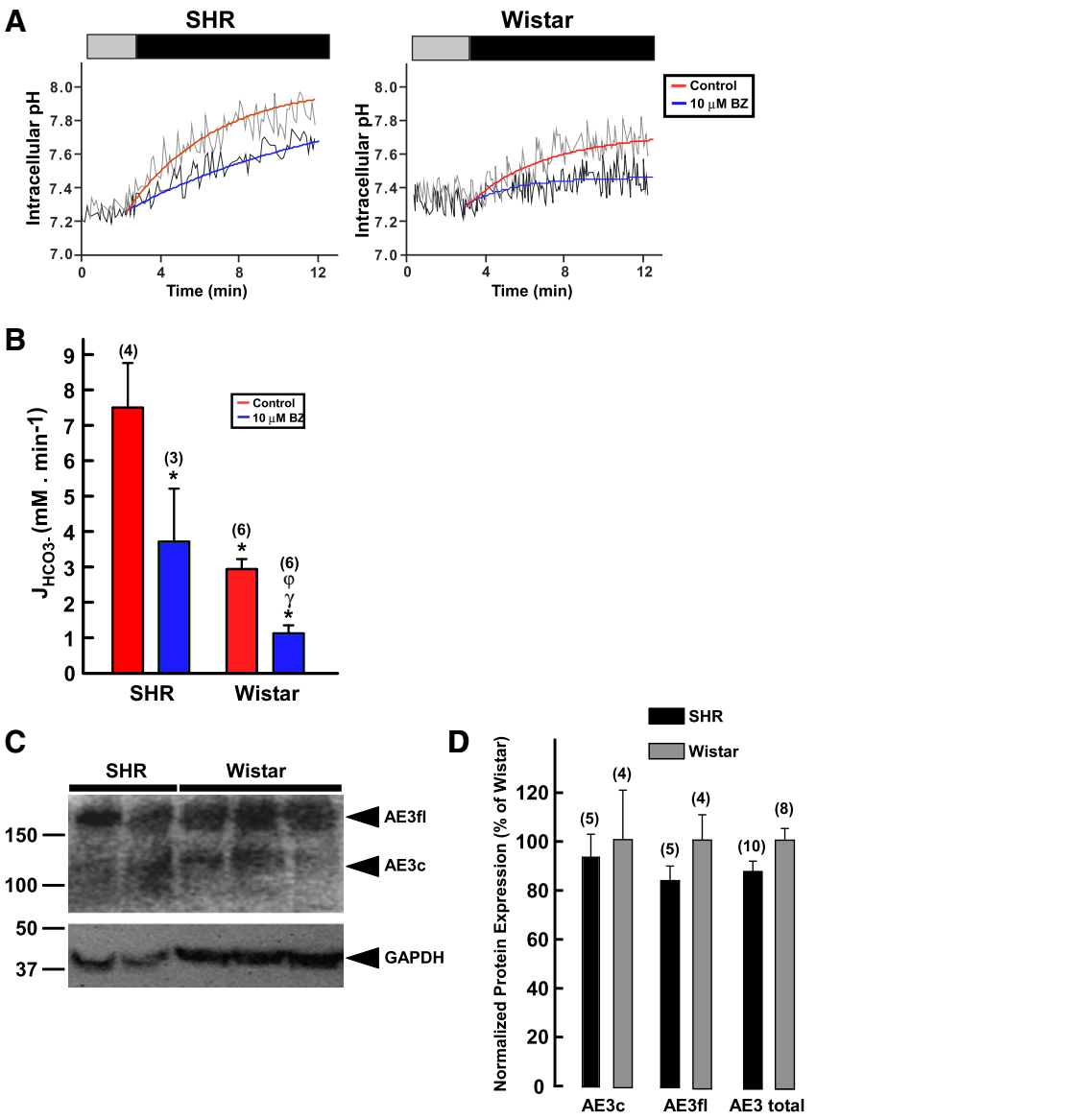

Fig. 6. Effect of carbonic anhydrase inhibition on cardiomyocyte Cl^-/HCO_3^- exchange activity, and expression of AE3fl and AE3c proteins in adult SHR and Wistar rat hearts. A, Examples of single SHR myocyte (left panel) and Wistar rat myocyte (right panel) used for pH_i measurement experiments. Cardiac myocytes were loaded with BCECF pH-sensitive fluorescent dye to measure pH_i. SHR and Wistar myocytes were perfused with either Cl^--containing (gray bar) or Cl^--free (black bar) buffer (gray traces, red lines). Separate experiments were performed in SHR and Wistar myocytes preincubated (20 min) with the carbonic anhydrase inhibitor, benzolamide (BZ 10 μM, black traces, blue lines) and exposed to Cl^--containing Cl^--free buffer. B, Summary of mean values of transport rates of SHR and Wistar control cardiomyocytes (no treatment, red bars), or cardiomyocytes treated with 10 μM BZ (blue bars). $^*p$ value<0.05, versus control group. $^*p<0.05$ vs. SHR (control), $^\gamma p<0.05$ vs. Wistar (control), and $^\varphi p<0.05$ vs. SHR (10 μM BZ) (ANOVA and Bonferroni's Multiple Comparison post-test analysis). Bracket at the top of the bar indicates the number of heart analyzed (2 cardiomyocytes analyzed in each heart). C, Whole lysates were prepared from hypertrophic (SHR) or normal (Wistar) adult rat heart ventricles. Protein samples (200 μg) were subjected to SDS-PAGE analysis, transferred to PVDF membrane, and probed with anti-AE3 (SA8) (top panel) and anti-GAPDH antibodies (bottom panel). Filled arrow indicates position of protein. D, Summary of the normalized protein values expressed relative to the Wistar heart protein expression. Bracket at the top indicates the number of hearts analyzed.

[16]. Enhanced Cl^-/HCO_3^- exchange activity in HEK293 cells co-expressing AE3fl–HA–CAXIV was prevented by BZ (3.8 ± 1.9 mM $H^+.min^{-1}$, n = 7), demonstrating a functional coupling between AE3 and CAXIV. To further examine whether bound CAXIV is necessary to maximize AE3-mediated Cl^-/HCO_3^- exchange activity, we coexpressed a functionally deficient CAXIV mutant and AE3fl–HA in HEK293 cells. Previously, the functionally inactive V143Y CAII failed to increased transport activity by the AE1 Cl^-/HCO_3^- exchanger [19,21]. The catalytically inactive CAXIV reduced transport activity by AE3fl–HA in cells coexpressing AE3fl–HA and CAXIV V159Y mutant (2.2 ± 0.2 mM $H^+.min^{-1}$, n = 5), compared to HEK cells expressing AE3fl–HA alone (Fig. 7C), demonstrating that formation of the complex is important to AE3 transport function.

Slc26a6 is the predominant Cl^-/HCO_3^- exchanger of the mouse heart [9], and clearly identified in the rat heart (Fig. 1C). Although SLC26A6 is not physically associated with CAXIV (Fig. 1) we want to eliminate the potential functional CAXIV-mediated effect on the Cl^-/HCO_3^- exchange activity by other transporters rather than AE3, in the rat myocardium. SLC26A6 Cl^-/HCO_3^- exchange activity was comparable to AE3fl–HA, when expressed in HEK cells (2.90 ± 0.6 mM $H^+.min^{-1}$, n = 5). However, CAXIV failed to increase transport activity by SLC26A6 in cells transiently coexpressing both SLC26A6 and CAXIV proteins (3.2 ± 0.6 mM $H^+.min^{-1}$, n = 4) (data not shown). We conclude that of the two main Cl^-/HCO_3^- exchangers expressed in rodent heart, AE3 and SLC26A6, only AE3 is receptive to the CAXIV stimulatory effect.

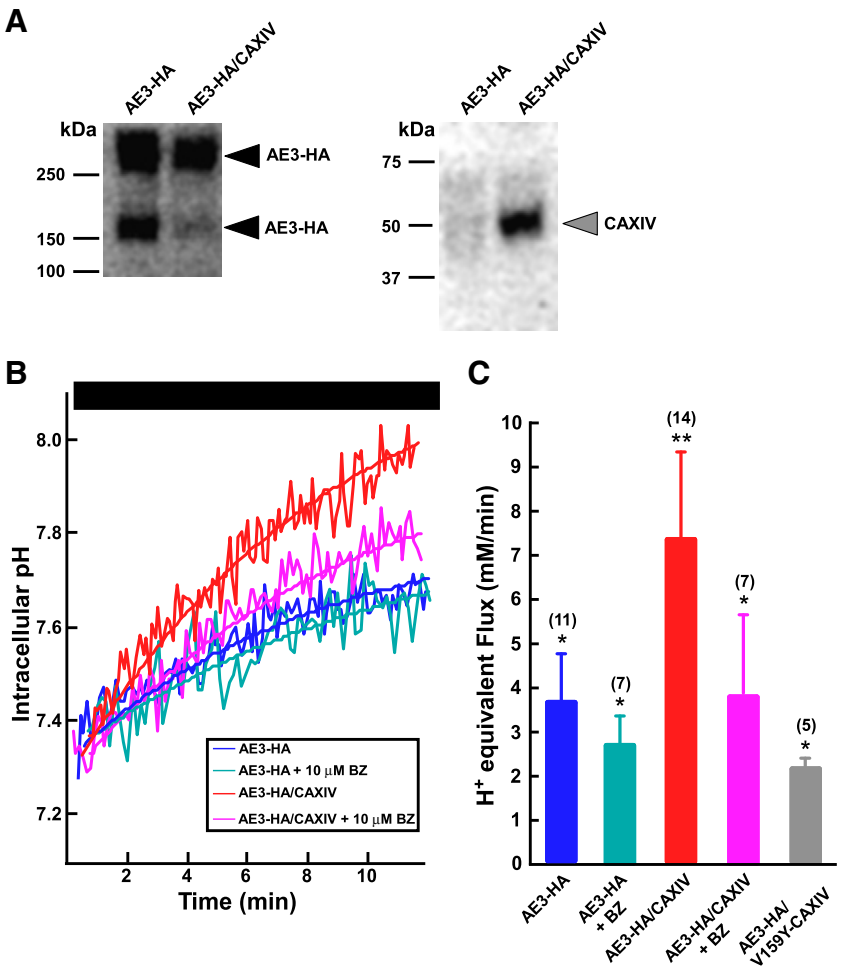

Fig. 7. Effect of carbonic anhydrase inhibition on AE3 and AE3/CAXIV transport activity. A, Lysates prepared from HEK293 cells transfected with AE3–HA cDNA (lane 1), or co-transfected with AE3fl–HA and CAXIV cDNAs (lane 2), were immunoblotted and probed for the expression of AE3fl–HA (left) or CAXIV (right). B, HEK293 cells transiently transfected with AE3fl–HA cDNA, or cotransfected with AE3fl–HA and CAXIV, cDNAs, were loaded with BCECF-AM and placed into a fluorimeter to monitor pH_i. Cells were maintained in a Cl^--containing buffer placed into a cuvette and continuously perfused with a Cl^--free buffer (black bar), in the presence or absence of 10 μM Benzolamide (BZ), as indicated. Initial rates of change of pH_i during the first minute were estimated from the slope of the line fitted by least squares method (straight lines). C, Summary of transport activity for HEK293 cells expressing AE3fl–HA, or coexpressing AE3fl–HA and CAXIV, or coexpressing AE3–HA and the catalytically inactive V159Y CAXIV mutant, as indicated. Transport activity of cells expressing AE3fl–HA, or AE3fl–HA and CAXIV, or AE3fl–HA and CAXIV–V159Y was normalized to the amount of AE3fl–HA protein expression. Some rates represent data collected in the presence of 10 μM Benzolamide (BZ), as indicated. Statistical significance was determined by ANOVA and Newman–Keuls Multiple Comparison post-test analysis. $^*p<0.05$ compared with AE3fl–HA/CAXIV. $^{**}p<0.05$ compared with AE3fl–HA. Bracket on top of the bars indicates number of experiments.

On the basis of these results, we propose that CAXIV functionally interacts with AE3, forming an extracellular membrane protein complex involved in the regulation of bicarbonate metabolism and pH_i in the heart. Increased CAXIV expression and consequent AE3/CAXIV complex formation would render the AE3 hyperactive in the hypertrophic myocardium of SHR.

4. Discussion

Bicarbonate metabolism and transport are key elements of cardiac function. In the present paper we have demonstrated a role played by the AE3 Cl^-/HCO_3^- exchanger and the CAXIV enzyme interaction in the heart. CAXIV bound to and enhanced Cl^-/HCO_3^- exchange activity of AE3, establishing a physical and functional coupling. Coimmunoprecipitation experiments demonstrated structural association of AE3 and CAXIV, when lysates of mouse and rat heart muscle were immunoprecipitated with specific goat anti-CAXIV antibody, and the complex formed detected with rabbit anti-AE3 antibody. Mice with targeted disruption of the *slc4a3* gene (*ae3*$^{-/-}$) were devoid of the AE3–CAXIV interaction, as demonstrated by coimmunoprecipitation experiments. Finally, both AE3 and CAXIV proteins colocalized in isolated adult mouse cardiomyocyte and ventricular sections, at the sarcolemma. Notably, the hypertrophic myocardium of SHR presented elevated expression of CAXIV with concomitant increased AE-mediated HCO_3^- fluxes, which were normalized to normal heart HCO_3^- fluxes by the membrane-impermeable CA inhibitor, BZ.

AE1 and AE3 members of the Slc4a family have been found in adult cardiomyocyte [8,35]. AE1 and AE3 bound to cytoplasmic (CAII) and GPI-linked (CAIV) CA enzymes, outlining physical/functional metabolon systems [41]. More recently, Slc26a6, the predominant Cl^-/HCO_3^- and Cl^-/OH^- exchanger of the mouse heart [9], was also found to bind cytoplasmic CAII, forming a different BTM [36]. Interestingly, Slc26a6/CAII interaction is regulated by protein kinase C (PKC). Phosphorylation of SLC26A6 by PKC decreases CAII/SLC26A6 interaction, reducing HCO_3^- transport by Slc26a6 and supporting a unique mechanism for acute regulation of membrane transport [36]. Herein, we have demonstrated a physical interaction of transmembrane CAXIV with both AE3c and AE3fl cardiac isoforms but not Slc26a6, in the mouse ventricle. In addition, PKC mediates the AE3-dependent increased anion exchange activity in the myocardium suggesting a role for AE3 in the development of cardiac hypertrophy [22,27].

The hypertrophic myocardium of SHR exhibited elevated NHE1-mediated Na^+/H^+ exchange activity compensated by enhanced AE3-mediated Cl^-/HCO_3^- exchange activity [14]. Combined action of AE3 and NHE1 would likely result in net cellular NaCl loading, without change of pH_i in the SHR myocardium, and in pro-hypertrophically-stimulated cardiomyocytes [22,23]. Moreover, the hypertrophic SHR have higher plasma AngII levels than WKY rats [42] that would drive the hyperactivation of AE3. Convincingly, angiotensin-converting enzyme (ACE) inhibition normalizes the enhanced activity of both AE3 and NHE1 exchangers while regressing cardiac hypertrophy, in SHR rats treated with the ACE inhibitor enalapril [15].

Recently, we found that the activity of AE3 and NHE1 promotes hypertrophy and the hypertrophy-programmed increases expression of the CA enzymes in cultured rat cardiomyocytes subjected to stimulation with AngII and the α-adrenergic agonist, phenylephrine [43]. Elevation of the CAII gene has been reported in rats with spontaneous hypertension and failing heart [44]. Furthermore, transgenic mice that develop AngII-mediated cardiac hypertrophy and dilated cardiomyopathy with aging showed increased expression of CAII, CAIV, CAVI, and CAXIV, mRNA, in addition to the inactive CA form, CAVIII [45]. CAII and CAIV mRNA levels rise in hypertrophied and failing human hearts, supporting the notion that CAII/CAIV activation is a component of the hypertrophic pathway (Alvarez BV et al., unpublished observations). Therefore, both hormonal-stimulated culture ventricular myocytes [43] and human hearts with signs of hypertrophy or failure showed amplified expression of CA genes.

The poorly membrane-permeable CA inhibitor, BZ, abolished the increase Cl^- dependant HCO_3^- fluxes mediated by anion exchangers in the hypertrophic SHR heart. Since SHR showed elevated CAXIV expression without alterations of the other CAs present in the myocardium (Figs. 4 and 5), or without modifications of the expression of myocardial AE3 proteins (AE3c and AE3fl, Figs. 6C, D), we speculate that BZ blocked primarily CAXIV, preventing the Cl^-/HCO_3^- exchange by AE3 (Fig. 8). Inhibition of AE-mediated Cl^-/HCO_3^- exchange in the normal myocardium by BZ proved that the AE function is dependent of the extracellular CA catalytic activity. Since AE3 associate with CAIV and CAIX [16,41], we cannot exclude that BZ is also inhibiting the CAIV/AE3 and CAIX/AE3 metabolons. On the other hand, BZ inhibited both CAIV and CAXIV in hippocampal neurons, proving that both CA enzymes play important roles in the regulation of intracellular pH in the brain by facilitating AE3-mediated Cl^-/HCO_3^- exchange [18]. In mouse muscle fibers, CAXIV account for almost 70% of total CA activity at the SL membrane [39], being CAIV responsible for the rest 30% CA activity [39,46]. In contrast, CAIX, contributes only to the registered t-tubular CA-activity of skeletal muscle, but not to the SL CA-activity [46]. In this line, maximization of the AE3-mediated HCO_3^- fluxes at the SL membrane of cardiac muscle by CA might be primarily due to CAXIV activity.

We propose that CAXIV form a tight functional complex with both AE3c and AE3fl transcripts. The mechanism by which transmembrane CAXIV regulate pH_i in cardiomyocytes occurs through the efficient removal of HCO_3^- locally formed in the vicinity of the AE3 Cl^-/HCO_3^- exchanger by the CA enzymatic activity, providing a local change of HCO_3^- gradient. In addition, other bicarbonate transporters expressed in cardiac muscle would bind to CAXIV forming other BTM and contributing to pH_i regulation in the heart (Fig. 8). Additional in vivo experiments which corroborate this hypothesis, however, have not been explored in the present manuscript. In an attempt to address how CAXIV mechanistically stimulates AE3 activity we coexpressed both AE3 and CAXIV proteins in the HEK cells system. In transfected HEK293 cells, BZ blocked the effect of CAXIV on AE3-mediated HCO_3^- fluxes (Figs. 7B, C). However, BZ did not inhibit the effect of endogenous CAII on AE3-mediated HCO_3^- fluxes. Given that CAII is intracellularly distributed [43], this suggests that the poorly membrane-permeable BZ at the concentration used in these experiments did not disrupt intracellular CA effects (Figs. 7B, C). We are aware that functional studies on HEK cells maintained under constant perfusion could dissipate any extracellular CA-mediated altered extracellular pH or gradient. However, we found that the catalytically inactive V159Y CAXIV mutant failed to increase Cl^-/HCO_3^- exchanger by AE3fl, when both proteins were transiently coexpressed in HEK cells (Fig. 7C). Therefore, we believe that only a bound and functionally extracellular CAXIV enzyme, which dissipates a local HCO_3^- gradient produced by the action of AE3, is the unique prerequisite for the CA-effect on AE3.

We previously demonstrated that tethering of CAII to AE3 increases the transmembrane HCO_3^- gradient local to AE3, thereby activating transport rate [19]. Linkage of AE3 Cl^-/HCO_3^- exchanger and CAXIV evolves as an efficient mechanism for HCO_3^- homeostasis and regulation of pH in the heart (Fig. 8). Yet, increased CAXIV expression in the hypertrophic heart of SHR alters the AE3-mediated HCO_3^- transport, creating a feed-forward cascade that would prompt an ionic imbalance. As speculated before, co-activation of NHE1 with AE3 in SHR would load cardiomyocytes with Na^+. The AngII-

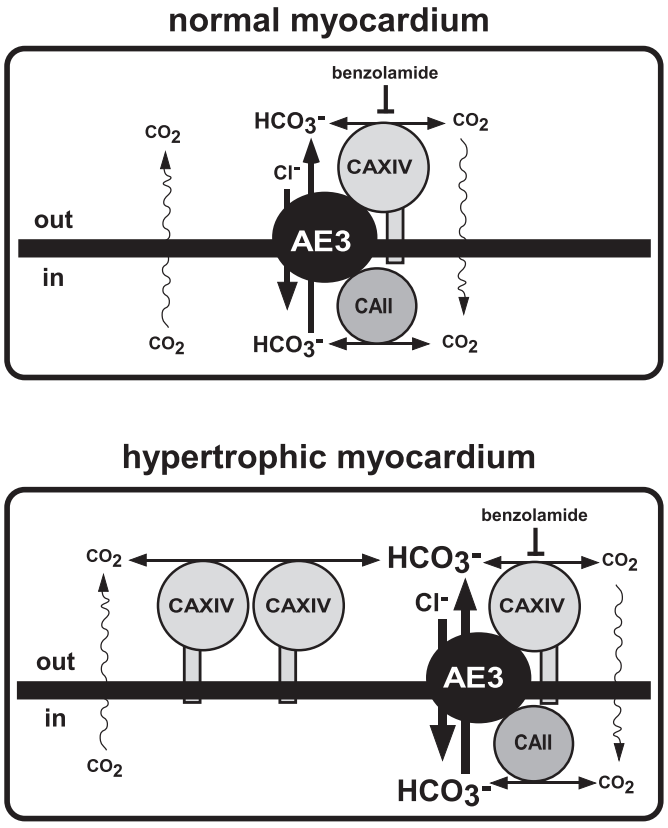

Fig. 8. Schematic model of the effect of CAXIV on AE3-mediated Cl^-/HCO_3^- exchange in the normal and hypertrophic myocardium. CAXIV form a tight functional complex with AE3. The mechanism by which transmembrane CAXIV with an extracellular catalytic domain regulate pH_i in cardiomyocytes, occurs through the efficient removal of HCO_3^- locally formed in the vicinity of the AE3 Cl^-/HCO_3^- exchanger by the CA enzymatic activity, providing a local change of HCO_3^- gradient. In the normal myocardium, the multi-molecular arrangement potentiates the Cl^-/HCO_3^- exchange activity by the production and removal of bicarbonate from the transport site. CAII and CAXIV cooperate to push bicarbonate to the transport site and then pull from the opposite side of the membrane [19,21] (top panel). In the hypertrophic myocardium, CAXIV protein expression increased and consequently favored the AE3/CAXIV complex formation which would increase the AE3 activity (bottom panel). Benzolamide, a poorly membrane-permeant CA inhibitor diminished the Cl^-/HCO_3^- exchange in the normal myocardium, proving the dependence upon extracellular CA of Cl^-/HCO_3^- exchange by AE3. Furthermore, BZ reduced the elevated Cl^-/HCO_3^- exchange activity observed in the hypertrophic heart. Contorted arrows show free diffusive movement of CO_2 across the plasma membrane of cardiomyocytes.

activated [22,27] and CAXIV-activated AE3 anion exchange activity in SHR would compensate for the enhanced NHE1 activity, blunting changes in the pH_i [14]. However, the increased $Na^+{}_i$ detected in the hypertrophic myocardium of SHR [47] may still be present even in the absence of changes of myocardial pH_i [14]. Increased $Na^+{}_i$ would lead to a secondary increase in $[Ca^{2+}]_i$ through the Na^+/Ca^{2+} (NCX) exchanger mechanism. Thus, changes in Ca^{2+} homeostasis which underlies NHE1/AE3 co-activation in SHR presumably through calcineurin/NFAT pathway, is a crucial factor contributing to the pathogenesis of the cardiac hypertrophy [48]. Interruption of the AE3/CAXIV complex formation in SHR might be a stage to prevent the hypertrophic growth of the heart.

Disclosures

None.

Acknowledgments

We thank Dr. Seth Alper (Beth Israel Deaconess Medical Center, Harvard Medical School, USA) for the AE3 (SA8) antibody and Dr. Joseph Casey (University of Alberta, Canada) for helpful comments. Dr. E. R. Swenson (University of Washington, Seattle, WA) kindly provided us with benzolamide. We also thank Dr. William Sly (Saint Louis University, MO) for the provision of the CAXIV mutant cDNA. This work was supported by the Agencia Nacional de Promoción Científica Grant (PICT 2007 No. 01011, Res. No. 320/08) to BVA. BVA is an Established Investigator of the Consejo Nacional de Investigaciones Científicas y Técnicas (CONICET, Argentina).

References

[1] Vaughan-Jones RD, Spitzer KW, Swietach P. Intracellular pH regulation in heart. J Mol Cell Cardiol 2009 Mar;46(3):318–31.
[2] Fabiato A, Fabiato F. Effects of pH on the myofilaments and the sarcoplasmic reticulum of skinned cells from cardiac and skeletal muscles. J Physiol 1978;276:233–55.
[3] Orchard CH, Kentish JC. Effects of changes of pH on the contractile function of cardiac muscle. Am J Physiol 1990;27:C967–81.
[4] Kramer BK, Smith TW, Kelly RA. Endothelin and increased contractility in adult rat ventricular myocytes. Role of intracellular alkalosis induced by activation of the protein kinase C-dependent Na^+–H^+ exchanger. Circ Res 1991 Jan;68(1):269–79.
[5] Kopito RR. Molecular biology of the anion exchanger gene family. Int Rev Cytol 1990;123:177–99.
[6] Cordat E, Casey JR. Bicarbonate transport in cell physiology and disease. Biochem J 2009;417(2):423–39.
[7] Su YR, Klanke CA, Houseal TW, Linn SC, Burk SE, Varvil TS, et al. Molecular cloning and physical and genetic mapping of the human anion exchanger isoform 3 (SLC2C) gene to chromosome 2q36. Genomics 1994 Aug;22(3):605–9.
[8] Alvarez BV, Kieller DM, Quon AL, Robertson M, Casey JR. Cardiac hypertrophy in anion exchanger 1-null mutant mice with severe hemolytic anemia. Am J Physiol 2007;292(3):H1301–12.
[9] Alvarez BV, Kieller DM, Quon AL, Markovich D, Casey JR. Slc26a6: a cardiac chloride-hydroxyl exchanger and predominant chloride-bicarbonate exchanger of the mouse heart. J Physiol 2004 Dec 15;561(Pt 3):721–34.
[10] Niederer SA, Swietach P, Wilson DA, Smith NP, Vaughan-Jones RD. Measuring and modeling chloride-hydroxyl exchange in the guinea-pig ventricular myocyte. Biophys J 2008 Mar 15;94(6):2385–403.
[11] Xu P, Spitzer KW. Na-independent Cl–HCO_3^- exchange mediates recovery from alkalosis in guinea pig ventricular myocytes. Am J Physiol 1994;267:H85–91.
[12] Leem CH, Lagadic-Gossmann D, Vaughan-Jones RD. Characterization of intracellular pH regulation in the guinea-pig ventricular myocyte. J Physiol 1999;517(Pt 1):159–80.
[13] Vandenberg JI, Metcalfe JC, Grace AA. Mechanisms of pHi recovery after global ischemia in the perfused heart. Circ Res 1993;72:993–1003.
[14] Perez NG, Alvarez BV, de Hurtado MC Camilion, Cingolani HE. pH_i regulation in myocardium of the spontaneously hypertensive rat. Compensated enhanced activity of the Na^+–H^+ exchanger. Circ Res 1995;77(6):1192–200.
[15] Ennis IL, Alvarez BV, de Hurtado MC Camilion, Cingolani HE. Enalapril induces regression of cardiac hypertrophy and normalization of pH_i regulatory mechanisms. Hypertension 1998;31(4):961–7.
[16] Morgan PE, Pastorekova S, Stuart-Tilley AK, Alper SL, Casey JR. Interactions of transmembrane carbonic anhydrase, CAIX, with bicarbonate transporters. Am J Physiol Cell Physiol 2007 Aug;293(2):C738–48.
[17] McMurtrie HL, Cleary HJ, Alvarez BV, Loiselle FB, Sterling D, Morgan PE, et al. The bicarbonate transport metabolon. J Enzyme Inhib Med Chem 2004 Jun;19(3):231–6.
[18] Svichar N, Waheed A, Sly WS, Hennings JC, Hubner CA, Chesler M. Carbonic anhydrases CA4 and CA14 both enhance AE3-mediated Cl–HCO_3^- exchange in hippocampal neurons. J Neurosci 2009 Mar 11;29(10):3252–8.
[19] Casey JR, Sly WS, Shah GN, Alvarez BV. Bicarbonate homeostasis in excitable tissues: role of AE3 Cl^-/HCO_3^- exchanger and carbonic anhydrase XIV interaction. Am J Physiol Cell Physiol 2009 Nov;297(5):C1091–102.
[20] Scheibe RJ, Gros G, Parkkila S, Waheed A, Grubb JH, Shah GN, et al. Expression of membrane-bound carbonic anhydrases IV, IX, and XIV in the mouse heart. J Histochem Cytochem 2006;54(12):1379–91.
[21] Sterling D, Reithmeier RA, Casey JR. A transport metabolon. Functional interaction of carbonic anhydrase II and chloride/bicarbonate exchangers. J Biol Chem 2001;276(51):47886–94.
[22] de Hurtado MC Camilion, Alvarez BV, Perez NG, Ennis IL, Cingolani HE. Angiotensin II activates Na^+-independent Cl^-–HCO_3^- exchange in ventricular myocardium. Circ Res 1998;82(4):473–81.
[23] de Hurtado MC Camilion, Alvarez BV, Ennis IL, Cingolani HE. Stimulation of myocardial Na^+-independent Cl^-–HCO_3^- exchanger by angiotensin II is mediated by endogenous endothelin. Circ Res 2000 Mar 31;86(6):622–7.
[24] Prasad V, Bodi I, Meyer JW, Wang Y, Ashraf M, Engle SJ, et al. Impaired cardiac contractility in mice lacking both the AE3 Cl^-/HCO_3^- exchanger and the NKCC1 Na^+–K^+–$2Cl^-$ cotransporter: effects on Ca^{2+} handling and protein phosphatases. J Biol Chem 2008 Nov 14;283(46):31303–14.
[25] Parkkila S, Parkkila AK, Rajaniemi H, Shah GN, Grubb JH, Waheed A, et al. Expression of membrane-associated carbonic anhydrase XIV on neurons and axons in mouse and human brain. Proc Natl Acad Sci U S A 2001 Feb 13;98(4):1918–23.
[26] Sterling D, Casey JR. Transport activity of AE3 chloride/bicarbonate anion-exchange proteins and their regulation by intracellular pH. Biochem J 1999;344(Pt 1):221–9.
[27] Alvarez BV, Fujinaga J, Casey JR. Molecular basis for angiotensin II-induced increase of chloride/bicarbonate exchange in the myocardium. Circ Res 2001 Dec 7;89(12):1246–53.
[28] Ruetz S, Lindsey AE, Ward CL, Kopito RR. Functional activation of plasma membrane anion exchangers occurs in a pre-Golgi compartment. J Cell Biol 1993;121(1):37–48.
[29] Loffing J, Moyer BD, Reynolds D, Shmukler BE, Alper SL, Stanton BA. Functional and molecular characterization of an anion exchanger in airway serous epithelial cells. Am J Physiol 2000 Oct;279(4):C1016–23.
[30] Aiello EA, Cingolani HE. Angiotensin II stimulates cardiac L-type Ca^{2+} current by a Ca^{2+}- and protein kinase C-dependent mechanism. Am J Physiol Heart Circ Physiol 2001 Apr;280(4):H1528–36.
[31] De Giusti VC, Correa MV, Villa-Abrille MC, Beltrano C, Yeves AM, de Cingolani GE, et al. The positive inotropic effect of endothelin-1 is mediated by mitochondrial reactive oxygen species. Life Sci 2008 Aug 15;83(7–8):264–71.
[32] Roos A, Boron WF. Intracellular pH. Physiol Rev 1981;61(2):296–434.
[33] Villa-Abrille MC, Cingolani E, Cingolani HE, Alvarez BV. Silencing of cardiac mitochondrial NHE1 prevents mitochondrial permeability transition pore opening. Am J Physiol Heart Circ Physiol 2011 Apr;300(4):H1237–51.
[34] Linn SC, Kudrycki KE, Shull GE. The predicted translation product of a cardiac AE3 mRNA contains an N-terminus distinct from that of the brain AE3 Cl^-/HCO_3^- exchanger. J Biol Chem 1992;267(11):7927–35.
[35] Puceat M, Korichneva I, Cassoly R, Vassort G. Identification of band 3-like proteins and Cl^-/HCO_3^- exchange in isolated cardiomyocytes. J Biol Chem 1995 Jan 20;270(3):1315–22.
[36] Alvarez BV, Vilas GL, Casey JR. Metabolon disruption: a mechanism that regulates bicarbonate transport. EMBO J 2005 Jul 20;24(14):2499–511.
[37] Chiappe de Cingolani G, Morgan P, Mundina-Weilenmann C, Casey J, Fujinaga J, Camilion de Hurtado M, et al. Hyperactivity and altered mRNA isoform expression of the Cl^-/HCO_3^- anion-exchanger in the hypertrophied myocardium. Cardiovasc Res 2001 Jul;51(1):71–9.
[38] Shah GN, Ulmasov B, Waheed A, Becker T, Makani S, Svichar N, et al. Carbonic anhydrase IV and XIV knockout mice: roles of the respective carbonic anhydrases in buffering the extracellular space in brain. Proc Natl Acad Sci U S A 2005 Nov 15;102(46):16771–6.
[39] Wetzel P, Scheibe RJ, Hellmann B, Hallerdei J, Shah GN, Waheed A, et al. Carbonic anhydrase XIV in skeletal muscle: subcellular localization and function from wild-type and knockout mice. Am J Physiol Cell Physiol 2007 Jul;293(1):C358–66.
[40] Svichar N, Esquenazi S, Waheed A, Sly WS, Chesler M. Functional demonstration of surface carbonic anhydrase IV activity on rat astrocytes. Glia 2006 Feb;53(3):241–7.
[41] Sterling D, Alvarez BV, Casey JR. The extracellular component of a transport metabolon. Extracellular loop 4 of the human AE1 Cl^-/HCO_3^- exchanger binds carbonic anhydrase IV. J Biol Chem 2002 Jul 12;277(28):25239–46.
[42] Yoneda M, Sanada H, Yatabe J, Midorikawa S, Hashimoto S, Sasaki M, et al. Differential effects of angiotensin II type-1 receptor antisense oligonucleotides on renal function in spontaneously hypertensive rats. Hypertension 2005 Jul;46(1):58–65.
[43] Alvarez BV, Johnson DE, Sowah D, Soliman D, Light PE, Xia Y, et al. Carbonic anhydrase inhibition prevents and reverts cardiomyocyte hypertrophy. J Physiol 2007;579(Pt 1):127–45.
[44] Sharkey LC, McCune SA, Yuan O, Lange C, Fray J. Spontaneous pregnancy-induced hypertension and intrauterine growth restriction in rats. Am J Hypertens 2001;14(10):1058–66.

[45] Domenighetti AA, Smyth G, Pedrazzini T, Proietto J, Delbridge LM. Gene expression profiling reveals distinct sets of genes altered during hormonally and metabolically induced cardiac hypertrophies. J Mol Cell Cardiol 2004;37:303.
[46] Hallerdei J, Scheibe RJ, Parkkila S, Waheed A, Sly WS, Gros G, et al. T tubules and surface membranes provide equally effective pathways of carbonic anhydrase-facilitated lactic acid transport in skeletal muscle. PLoS One 2010;5(12):e15137.
[47] Jelicks LA, Gupta RK. Nuclear magnetic resonance measurement of intracellular sodium in the perfused normotensive and spontaneously hypertensive rat heart. Am J Hypertens 1994 May;7(5):429–35.
[48] Ennis IL, Garciarena CD, Escudero EM, Perez NG, Dulce RA, de Hurtado MC Camilion, et al. Normalization of the calcineurin pathway underlies the regression of hypertensive hypertrophy induced by Na^+/H^+ exchanger-1 (NHE-1) inhibition. Can J Physiol Pharmacol 2007 Mar–Apr;85(3–4):301–10.